The spectral and beaming characteristics of the anomalous X-ray pulsar 4U 0142+61

J. E. Trümper[1], N. D. Kylafis[2,3], Ü. Ertan[4], and A. Zezas[2,3]

[1] Max-Planck-Institut für extraterrestrische Physik, Postfach 1312, 85741 Garching, Germany

[2] University of Crete, Physics Department & Institute of Theoretical & Computational Physics, 71003 Heraklion, Crete, Greece

[3] Foundation for Research and Technology-Hellas, 71110 Heraklion, Crete, Greece

[4] Faculty of Engineering and Natural Sciences, Sabancı University, 34956, Orhanlı, Tuzla, İstanbul, Turkey

Received ; accepted

ABSTRACT

Context. Anomalous X-ray pulsars (AXPs) and soft gamma-ray repeaters (SGRs) constitute a special population of young neutron stars, which are thought to be magnetars, i.e., neutron stars with super-strong magnetic fields ($10^{14} - 10^{15}$) G.
Aims. Assuming that AXPs and SGRs accrete matter from a fallback disk, we attempt to explain the energy-dependent pulse profiles exhibited by the AXP 4U 0142+61, as well as its phase-dependent energy spectra.
Methods. We test the hypothesis that not only the X-ray spectra, but also the energy-dependent pulse profiles of 4U 0142+61 are produced by accretion along dipole magnetic field lines of strength $10^{12} - 10^{13}$ G at the neutron-star surface.
Results. In the fallback disk model, the Thomson optical depth along the accretion funnel is significant and bulk-motion Comptonization operates efficiently. This is enhanced by resonant cyclotron scattering. The thus scattered photons escape mainly sideways and produce a fan beam, which is detected as a main pulse up to energies of ~ 160 keV. The approximately isotropic emission from the stellar surface (soft thermal photons and reflected hard X-ray ones) is detected as a secondary pulse. This secondary pulse shows a bump at an energy of about 60 keV, which may be interpreted as resonant cyclotron scattering of fan-beam photons at the neutron-star surface. This implies a dipole magnetic field strength $B \approx 7 \times 10^{12}(1 + z)$ G, where z is the gravitational redshift.
Conclusions. Our model explains not only the soft and hard X-ray spectra of the AXP 4U 0142+61, but also its energy dependent pulse profiles. If our interpretation of the energy dependence of the secondary pulse is correct, the surface dipole magnetic field strength is comparable to that of X-ray pulsars. Much like our Sun, the surface multipole magnetic field strength may be two orders of magnitude larger, thus allowing for energetic bursts to occur. The accretion process is mediated by the dipole field and is not interfering at all with the multipole field.

Key words. pulsars: individual (4U 0142+61) – X-rays: stars – stars: magnetic fields – accretion disks

1. Introduction

Anomalous X-ray pulsars (AXPs) and Soft Gamma Ray Repeaters (SGRs) are young neutron stars with X-ray luminosities much larger than their spin-down power and long periods in the range $2 - 12$ s. They are widely believed to be magnetars deriving their X-ray emission from the decay of super-strong magnetic fields ($\gtrsim 10^{15}$ G) (e.g. Duncan & Thompson 1992; Thompson & Duncan 1995). At the outset, the magnetar model was developed to explain the giant bursts and the large bursts of SGRs, which exceed the Eddington limit of neutron-star luminosities by a very large factor. If the observed spin-down of these sources is interpreted as the consequence of magnetic dipole braking, the resulting polar field strengths are of the order of $\gtrsim 10^{15}$ G, in qualitative agreement with what has been inferred from the observed luminosities (Kouveliotou et al. 1999). Later on, it was discovered that AXPs show short bursts as well, though less frequent and less energetic, leading to the gen-

eral notion that both types of sources are closely related or represent even a single class. In the magnetar picture, the steady X-ray emission of these sources, which have luminosities of typically a few times 10^{35} erg s^{-1}, is thought to be caused by a twist of the magnetosphere leading to the amplification of the magnetic field and the acceleration of particles, which produce the X-ray emission. The twist is caused by rotational motions of a crust plate and has a lifetime of $\gtrsim 1$ yr (Beloborodov & Thomson 2007). For recent reviews of the magnetar model see Woods & Thompson (2006) and Mereghetti (2008).

An alternative energy source for the persistent and transient X-ray luminosities of AXPs and SGRs is accretion from fallback disks, first proposed, but soon abandoned, by van Paradijs et al. (1995), followed by Chatterjee et al. (2000) and Alpar (2001). This class of models was developed further in a series of papers (Ekşi & Alpar 2003; Ertan & Alpar 2003; Ertan & Cheng 2004; Ertan et al.

2006; Ertan & Çalışkan 2006; Ertan et al. 2007; Ertan & Erkut 2008, Ertan et al. 2009), which make the fallback-disk idea quite attractive. The fallback-disk model gets support from the discovery of IR/optical radiation from two of the AXPs, 4U 0142+61 (Wang et al. 2006) and 1E 2259+586 (Kaplan et al. 2009), which has been successfully interpreted as disk emission. Further indirect support comes from the discovery of three planets orbiting a neutron star (Wolszczan & Frail 1992; Wolszczan 1995). The fallback-disk model explains the spin-down of AXPs and SGRs by the disk-magnetosphere interaction and requires only "normal" neutron-star dipole fields ($10^{12} - 10^{13}$ G). In addition, it is successful in predicting the period clustering of AXPs/SGRs in the range of $2-12$ s. On the other hand, this model cannot explain the super-Eddington bursts, which are relatively rare. They are attributed to magnetar-type activities occurring in local *multipole* fields (star-spots).

The main physical questions addressed in the present paper are:

1) What is the source of energy powering the persistent emission of these sources? Magnetic-field decay or accretion?

2) How large are the polar dipole-field strengths of these neutron stars? Are they super-strong ($\gtrsim 10^{15}$ G) or "normal" ($10^{12} - 10^{13}$ G)?

The spectra of AXPs and SGRs in the range $0.5 - 10$ keV have been modeled by a superposition of blackbody and power-law or, alternatively, double blackbody emission. Recently, hard X-ray tails at energies reaching up to more than 100 keV have been observed. For a recent review see Mereghetti (2008). The luminosities in these tails observed at energies $\gtrsim 20$ keV are of the same order as the soft X-ray luminosities, which is a challenge to any model. Very recently, Enoto et al. (2010) published a homogeneous set of data on 7 sources showing both soft and hard components, as well as their periods and period derivatives.

Using the bulk-motion and thermal Comptonization (BMC/TC) model of Farinelli et al. (2008), Trümper et al. (2010) have shown that accretion from a fallback disk can produce the hard X-ray ($\gtrsim 2$ keV) spectrum of 4U 0142+61. The mechanism operates close to the hot thermal mound near the bottom of the accretion column, where the free-falling matter is stopped. The required seed photons are produced in two places (see Fig. 1): a) The photosphere of the neutron star, which emits most of the low-energy photons in the $0.5 - 2$ keV range and b) the hot thermal mound at the bottom of the accretion column (e.g., Basko & Sunyaev 1976; Becker & Wolff 2007), which has a higher temperature than the photosphere. In the following, we discuss the formation of the different spectral components of 4U 0142+61 and show that not only the observed broad-band spectrum, but also the energy-dependent pulse profiles (den Hartog et al. 2008) can be explained by the BMC/TC model. In particular, we present evidence that the magnetic-dipole field at the surface of this neutron star is $\sim 8 \times 10^{12}$ G, consistent with the expectations of the fallback-disk model.

2. The model

In what follows, we give the basic picture that we have in mind, part of which was presented in Trümper et al. (2010). In particular, we discuss the geometrical constraints that
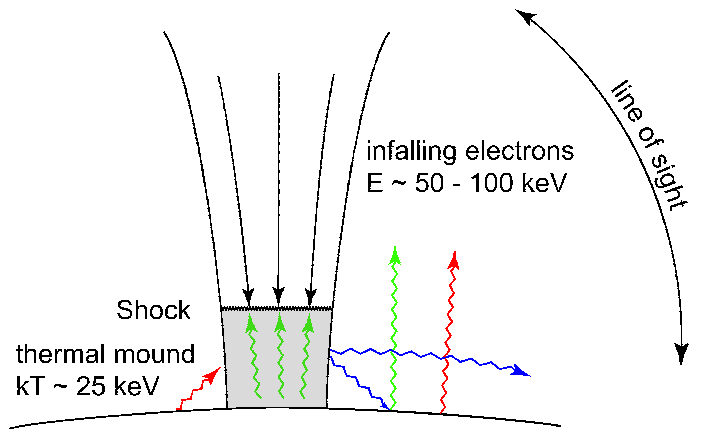

Fig. 1. Schematic description of the beaming pattern. The different wiggly arrows show the mean direction of the respective component. Blue: The fan beam (main pulse), consisting of photons with energies between ~ 2 and 160 keV, is produced by the BMC/TC process. It is subject to gravitational bending. Green: Fan-beam photons hitting the neutron-star photosphere will be reflected (scattered). Red: Soft photons from the photosphere escape, while a small fraction contributes as seed photons for the Comptonization process.

the observations of 4U 0142+61 place on the emission region and the accretion column and then we discuss the role that the dipole magnetic field plays in the formation of the X-ray spectrum and the energy-dependent pulse profiles.

2.1. Geometrical constraints for the emission region and optical depths

Fig. 1 shows a schematic picture of the X-ray emitting region. Following Trümper et al. (2010), we assume that the hard X-ray component ($2 - 160$ keV) is produced by thermal Comptonization (TC, $2-10$ keV) in the accretion shock and the hot mound at the bottom of the accretion funnel and bulk-motion Comptonization (BMC, $\gtrsim 10$ keV) in the accretion flow.

Despite the fact that the magnetic field plays a significant role in the radiative transfer (see Section 2.2 below), it is instructive to look at the Thomson optical depths involved in this problem. In the free-fall regime, the transverse Thomson optical depth τ_t in the direction perpendicular to the magnetic field, near the neutron-star surface, is

$$\tau_t = n_0 \sigma_T a_0 = \frac{\dot{M}}{m_p v_{ff} \pi a_0^2} \sigma_T a_0, \qquad (1)$$

where a_0 is the radius of the accretion funnel at the neutron-star radius, n_0 and v_{ff} are the electron density and the free-fall velocity at the bottom of the accretion funnel, $\dot{M}$ is the accretion rate, σ_T is the Thomson cross section, and m_p is the proton mass. For $\dot{M} \approx 2 \times 10^{15}$ g s^{-1} (corresponding to an X-ray luminosity of 3.7×10^{35} erg s^{-1}) and $v_{ff} \approx 0.5\ c$, we get for the transverse optical depth $\tau_t \approx 1.7 \times 10^4/a_0$, where a_0 is measured in cm. In order to have the BMC process work efficiently, the BMC region has to be moderately optically thick in the transverse direction, which implies that a_0 must be of the order of 100 m or less. On the other hand, the blackbody radius r_{bb} of the observed

soft component $(0.5 - 2)$ keV emitted by the photosphere is much larger. It was found to be 8.6 km (White et al. 1996), $5.4 - 8.3$ km (Israel et al. 1999) or 7.2 km (Juett et al. 2002). All these radii are normalized to a distance of 3.6 kpc.

In the direction parallel to the magnetic field the Thomson optical depth of the free-fall zone (the BMC zone) is

$$\tau_p = \frac{2}{3}\tau_t \frac{R}{a_0} \approx 1.1 \times 10^{10}/a_0^2. \tag{2}$$

For $a_0 \lesssim 100$ m, we obtain $\tau_p \gtrsim 100$. In this direction the Thomson optical depth is huge and the accreting matter acts like an impenetrable wall to the outgoing photons. Because of this, we can find an upper limit to the transverse Thomson optical depth τ_t as follows:

The hard X-ray spectrum, say from 10 to 100 keV, is produced by repeated "head-on" collisions (Mastichiadis & Kylafis 1992) between the photons that come out of the thermal mound and the infalling electrons, whose Lorentz γ is approximately 1.15 near the neutron-star surface. The number of such collisions required to upscatter an $E_i \sim 10$ keV photon to an $E_f \sim 100$ keV one is $N_{sc} \sim \log(E_f/E_i)/\log\gamma^2 \sim 8$. On the other hand, the observed photon-number spectral index of the hard X-rays is $\Gamma \approx 1$. This means that after each head-on collision, roughly 25% of the photons escape, while the rest suffer yet one more head-on collision with the infalling electrons.

Let now H be the mean free path of the outgoing thermally Comptonized photons in the infalling plasma close to the neutron-star surface. Then, $H \approx 1/(n_0\sigma_T) = a_0/\tau_t$. The upscattered photons escape sideways, through a cylindrical surface of height $\sim H$. The fractional solid angle that this surface subtends at the axis of the accretion funnel is $\Omega_{esc}/2\pi \sim H/a_0 \sim 1/\tau_t$. Equating this with the escape probability of ~ 0.25, we find $\tau_t \sim 4$.

2.2. The role of the dipole magnetic field

The Farinelli et al. (2008) BMC/TC mechanism applied by Trümper et al. (2010) has been designed for the non-magnetic case, since it is using Thomson cross sections. Since we assume that the polar magnetic fields of the AXPs and SGRs are of the order of $10^{12} - 10^{13}$ G, magnetic cross sections (e.g. Meszaros 1992) should be used. After the pioneering work of Basko & Sunyaev (1976), many people have worked in this area. Becker & Wolff (2005, 2007) have advanced this complicated undertaking by an analytical approach using angle averaged magnetic cross sections and a cylindrical approximation for the accretion column. However, their results are not directly applicable to AXPs/SGRs, because they have been obtained for sources like Her X-1 and LMC X-4, which have higher luminosities by more than a factor of a hundred.

The most important effect of the strong magnetic field is that the cross section of the extraordinary-mode photons is significantly different from the Thomson cross section. At photon energies E much smaller than the cyclotron energy $E_c = (h/2\pi)(eB/m_e c)$, the cross section becomes much smaller than σ_T for photons propagating parallel to the magnetic field, while it becomes very large close to the cyclotron resonance. These effects are softened somewhat by the effects of vacuum polarization and spin-flip scattering. We expect that the inclusion of the magnetic effects will

lead to a change of the values of the parameters a_0, τ_t, and τ_p (Section 2.1). However, the inclusion of these effects will not change the main result of Trumper et al. (2010), namely the fact that the broad-band $(0.5-200\,\text{keV})$ spectrum of 4U 0142+61 can be represented by a single physical model involving TC and BMC of photons by the infalling electrons. Any deviation from the geometry of the TC/BMC model of Farinelli et al. (2008) and the inclusion of effects due to a strong magnetic field will be absorbed in the values of the model parameters and as a result the later should not be taken at face value. We expect that the parameters related to the seed photon spectrum (temperature and slope of the modified blackbody, and the illumination factor) will be mostly affected by the change in the geometry discussed in Section 2.1 (Fig. 1).

Extraordinary photons of energy E will be scattered quasi-isotropically by electrons when passing sheets in which the resonance condition $E \approx E_c = \gamma(h/2\pi)(eB/m_e c)$ is fulfilled, where γ is the Lorentz factor of the electrons ($\gamma \approx 1.15$ for free-falling electrons near the neutron-star surface and $\gamma = 1$ for thermal electrons). For photons of energy E, the scattering sheet is located at a radius $r(E) = R(E_{c0}/E)^{1/3}$, where E_{c0} is the cyclotron resonance energy at the neutron-star surface.

The resonant scattering optical depth in the accretion column, parallel to the magnetic field, greatly exceeds the optical depth for Thomson scattering (Lyutikov & Gavriil 2006)

$$\tau_{res} \sim \frac{\pi c}{8 r_e \omega_c} \sim 10^5 \left(\frac{1\,\text{keV}}{E_c}\right), \tag{4}$$

where r_e is the classical electron radius, and ω_c, E_c are the cyclotron frequency and cyclotron energy, respectively. This means that, for photon energies in the range $0.2 - 160$ keV, cyclotron resonance scattering is the main source of opacity. In the "resonance layer", located at radius $r(E) \approx R(E_{c0}/E)^{1/3}$, photons of energy E are quasi-isotropically redistributed.

In addition, the scattering by the cyclotron harmonics has to be taken into account, which for a given photon energy E takes place at radii $r(E) \approx R(jE_{c0}/E)^{1/3}$, with $j = 2, 3, 4....$

Since the dipole magnetic field decreases rapidly in the vertical direction, the cyclotron scattering dominates over a wide range of photon energies and strongly prevents extraordinary photons from traveling upstream. At the same time, these scattering effects enhance the efficiency of the bulk-motion Comptonization process.

For extraordinary mode photons, traveling at small angles with respect to the magnetic field direction, with energies much smaller than the local cyclotron energy, the scattering cross section becomes much smaller than the Thomson value. This appears to have the opposite effect than the one discussed above. However, the extraordinary photons traveling upwards will eventually be stopped by cyclotron scattering when passing a resonance layer at higher heights.

On the other hand, the ordinary-mode photons also cannot escape in the magnetic field direction, because the Thomson optical depth τ_p is significantly larger than one and, in addition, the photons are advected downward by the accretion flow. Since τ_p is significantly larger than τ_t, nearly all the ordinary-mode photons escape sideways, i.e., perpendicular to the accretion flow. In view of the above,
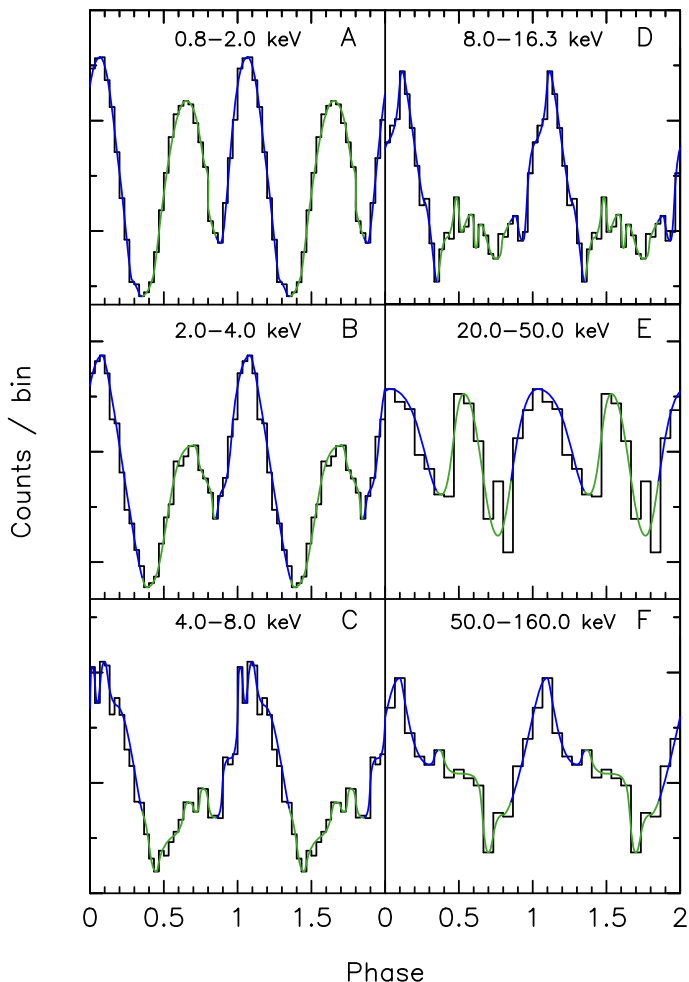
Fig. 2. Schematic presentation of the energy dependent pulse profiles measured by XMM-Newton, RXTE-PCA and INTEGRAL-ISGRI. The main pulse (blue phase) ranges from the lowest to the highest energies. In our model, this component is mainly formed by the fan-beam photons produced by the BMC/TC process. The secondary pulse (green phase) is produced by the photospheric radiation at low energies ($\lesssim 2$ keV) and the fan-beam photons, which hit the photosphere and are reflected there. The intensity of this pulse falls off quickly between 0.8 and 8 keV. It reappears at higher energies and becomes as prominent as the main pulse in the $16.3 - 50$ keV interval. This figure is a simplification of Fig. 7 of den Hartog et al. (2008).

we conclude that the column will largely emit a fan beam, as shown schematically in Fig. 1.

2.3. Interpretation of the 4U 0142+61 pulse shapes and energy spectra

A comprehensive and detailed description of the broadband X-ray characteristics of AXP 4U 0142+61 has been given by den Hartog et al. (2008). In the following, we present a detailed discussion of these results in terms of the accretion model. To this end, we use two results of the den Hartog et al. (2008) paper, the energy-dependent pulse profiles shown in Fig. 2, measured by XMM-Newton, RXTE-PCA, and INTEGRAL-ISGRI, and the complementary phase-dependent energy spectra shown in Fig. 3.
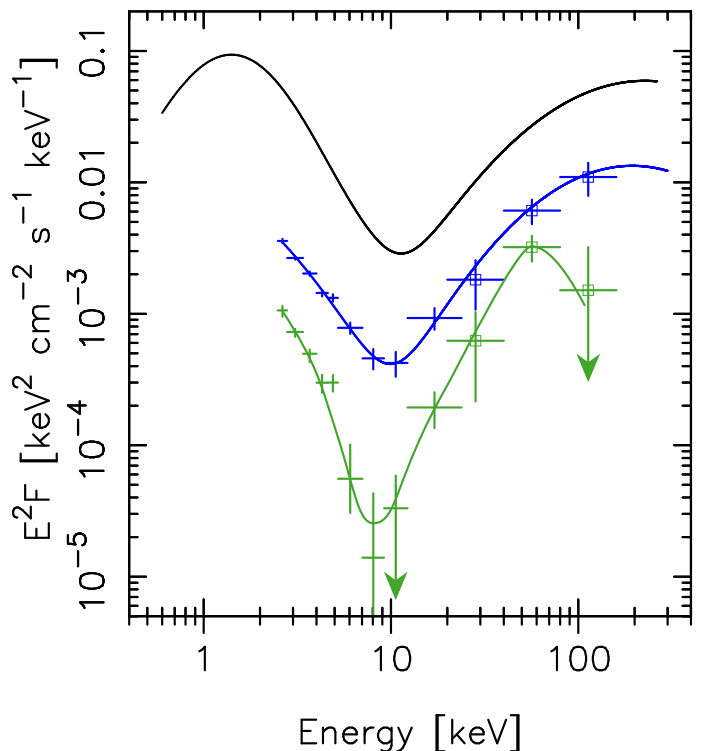

Fig. 3. This figure is a simplification of Fig. 8 of den Hartog et al. (2008), from which the data are taken. The black line represents the INTEGRAL/XMM-Newton total spectrum fit shown in that paper. The spectrum of the main pulse is shown in blue. The spectrum of the secondary pulse in shown in green. In our model, this component consists above ~ 8 keV of fan-beam photons reflected by the photosphere. Its spectrum shows a rapid rise up to energies of ~ 60 keV and a break at ~ 80 keV. In our model, this bump, which can also be seen in the pulse shapes (Fig. 2), is interpreted in terms of enhanced reflection due to cyclotron resonance scattering.

As noted by den Hartog et al. (2008), morphology changes are ongoing throughout the whole energy range. However, the principal structure of the pulse profiles is very simple: It mainly consists of two pulses (c.f. Fig. 2). In Figs. 2 and 3 we present simplified versions of the energy-dependent pulse profiles and the phase-dependent spectra, which are labeled by colors. The main pulse (blue color), peaking around phase 0.1, is located at a stable position from the lowest to the highest energies and the secondary pulse (green color) is located at phases around 0.6 (Fig. 2). The phase-dependent spectra (Fig. 3) show the same color.

2.3.1. Interpretation of the main pulse

The interpretation of the main pulse is very simple in our model. We identify it with the fan beam emitted from the region of the hot shock/mound and the infalling matter above it (Fig. 1). At the lowest energies ($E \lesssim 1.7$) keV, the emission consists of two components, the blackbody-like emission from the part of the extended photosphere that faces the observer and the low-energy tail of the BMC/TC spectrum that is emitted as a fan beam. In the energy interval $1.7 \lesssim E \lesssim 10$ keV, the spectrum is composed of the tail of the photospheric spectrum and the power-law spectrum

produced by the thermal Comptonization (TC). At energies $E \gtrsim 10$ keV, up to the highest energies beyond 100 keV, the emission is due to the bulk-motion Comptonization (BMC).

2.3.2. Interpretation of the secondary pulse

In Figs. 2 and 3 we show as green lines the secondary pulse, which occurs at phase ~ 0.6. We identify it with the polar beam (Fig. 1). As in the case of the main pulse, here also we consider three energy bands.

The intensity of the secondary pulse rises strongly towards low energies (Fig. 2). An extrapolation of the trend shows that at energies below 0.8 keV it becomes stronger than the main pulse, which is fully consistent with the ASCA data in the $0.5 - 1.7$ keV band (Kuiper et al. 2006; den Hartog et al. 2008). We interpret this component in terms of the blackbody-like spectrum dominating at energies below 2 keV and originating in the extended hot photosphere surrounding the accretion column, which has a rather large extent ($r_{bb} \sim 5 - 8$ km). The main difference in the angular distribution compared with that of a blackbody is that a broad peak occurs in the polar direction, caused by extraordinary photons escaping from larger depths (c.f. Pavlov et al. 1994). The emission from this area will be composed of an approximately isotropic component and a narrower pencil beam of extraordinary-mode photons, which escape from the deeper layers along the magnetic field lines.

In the $1.7 - 10$ keV band, the intensity of the secondary pulse falls off steeply with energy. In our model, this part of the spectrum is produced by the superposition of the tail of the blackbody distribution and the power-law spectrum produced by thermal Comptonization (TC). A possible third component can be produced by reflection of a fraction of fan-beamed TC photons, which hits the polar-cap area. The reflected photons leave the neutron-star surface more or less isotropically, i.e. with an angular distribution similar to that of the thermal emission from the photosphere. Thus, both components are in phase.

In the $10 - 50$ keV band, the secondary pulse becomes quite strong and it is actually comparable in strength with the main pulse. We note that this pulse extends into the $50 - 160$ keV energy band, where it is visible as a shoulder of the main pulse (Fig. 2). But the effect is small due to the large width of this energy interval. It can be seen better if one looks at the phase-resolved spectra shown in Fig. 3. The secondary pulse spectrum shows a broad bump in the $20 - 80$ keV range. Actually, its intensity rises faster than that of the main pulse up to an energy of ~ 60 keV, beyond which it indicates a drop. We will return to this feature in Section 3. In our model, this part of the spectrum is produced by the BMC photons that hit the neutron-star surface and get reflected (scattered) with some energy loss. Since the reflected photons have a more or less isotropic distribution in direction, this energy band is in phase with the previous two.

2.3.3. Remarks

Concluding our interpretation of the energy-dependent pulse shapes, we think it is appropriate to give some remarks:

1. In Fig. 1, we show the swing of the line of sight during half a phase cycle, approximately required by our model for 4U 0142+61, which ranges from a direction roughly perpendicular to the accretion column (main pulse) to an off-pole direction (secondary pulse). We stress that the phenomenological appearance of an AXP or SGR in terms of energy-dependent pulse shapes or phase-dependent spectra will depend crucially on this viewing geometry, which in turn depends on the angles between the rotational axis of the neutron star and the line of sight on one hand and the dipole axis, on the other.

2. The gravitational bending of the fan beam may play an important role for the beaming, depending on the unknown mass and radius of the neutron star.

3. As mentioned above, the hot polar cap has a radius $r_{bb} \sim 5 - 8$ km. The spectral fits of White et al. (1996), Israel et al. (1999), and Juet et al. (2002) yield a temperature of $kT \approx 0.4$ keV. However, this is probably a flux-averaged temperature, since the temperature will decrease from higher values close to the accretion column to lower values at larger distances.

4. The energy-dependent pulse shapes in Fig. 2 represent only the pulsed components without the constant components. The pulsed fractions can be found in Fig. 9 of den Hartog et al. (2008). They are quite low at soft energies ($\sim 10\%$ at 1 keV), which is qualitatively expected from our model, since the photosphere is visible to the observer all the time (see Fig. 1). On the other hand, the TC/BMC components show larger pulse fractions ($\sim 25\%$ above 28 keV), as anticipated for the dominating fan beam.

3. An estimate of the magnetic dipole field of AXP 4U 0142+61?

We believe that the dipole magnetic field is not only channeling the accretion flow onto the poles, but also leaves its imprint in the observed spectra. As already discussed above, the spectrum of the secondary (polar) beam is characterized by a fast rise (faster than that of the fan beam) from ~ 10 keV up to a maximum at ~ 60 keV, followed by a decline or a cutoff beyond ~ 70 keV. This behavior is expected if the polar beam is produced by scattering at the photospheric plasma, whose efficiency rises for energies approaching the cyclotron energy. Interpreting the spectrum this way, leads to a cyclotron energy of $70 - 80$ keV, corresponding to a polar magnetic field strength of $B_0 \sim 6 - 7 \times 10^{12}(1 + z)$ G, where z is the gravitational redshift. Clearly, observations with higher photon statistics would be necessary to confirm this conclusion.

4. Heating of the hot polar cap

The photosphere responsible for the soft component has a flux-averaged temperature of ~ 0.4 keV and a blackbody radius $r_{bb} \sim 5 - 8$ km. In our model, there are three possible ways to heat the polar cap:

1. By absorption of a fraction of the fan-beam photons hitting the neutron-star surface. This process will be enhanced by the gravitational bending of the fan beam towards the neutron-star surface, which depends on the gravity of the neutron star, i.e., its mass over its radius. If this were the main heat source of the polar cap, the power of the re-emitted thermal component and the reflected (scattered) component would be equal to the power of the fan beam impinging on the polar cap.

2. A second heat source may be that part of the accretional power which is conducted into the stellar interior and redistributed over a larger area, depending on the magnetic-field configuration in the interior and the crust.

3. Another contribution to the heating of the polar cap could be provided by conduction of heat from the hot interior of the relatively young neutron star.

In view of our limited quantitative understanding of all properties and processes, which play a role in this context, it would be premature to favor a specific combination of these processes.

5. Summary and conclusions

We have shown in a semi-quantitative way that bulk-motion/thermal Comptonization in an accretion column, formed by a dipole magnetic field of strength $\sim 10^{13}$ G, describes well not only the soft and hard X-ray spectra but also the phase-dependent energy spectra of AXP 4U 0142+61. The energy-dependent pulse profiles and their constancy over long periods of time constitute significant observational constraints for the proposed models. Our model explains them in a simple and natural way by the formation of two "beams", one perpendicular to the accretion column (main pulse) and one roughly parallel to it (secondary pulse). AXP 4U 0142+61 is one of seven sources presently known to have hard X-ray tails (Enoto et al. 2010). From the similarity of their broad-band spectra, it is no surprise that accretion with thermal and bulk-motion Comptonization works for all of them (Zezas et al., in preparation).

On the other hand, the magnetar model of a twisted magnetic field (Thompson et al. 2000), where the hard X-ray emission originates far up in the magnetosphere, seems to have problems in explaining the energy-dependent pulse profiles (Fernandez & Thompson 2007) Another problem for the magnetic-twist model is the long term stability of the pulse shape and phases. This would require that the rotation of the same crustal plate, located at a fixed position on the neutron star, is responsible for the quiescent emission, which looks quite artificial. Furthermore, the $\dot{P}$ of SGR 0418+5729 was determined (Rea et al. 2010) to be less than 6×10^{-15} s s^{-1}, which in the magnetar model implies a magnetic dipole field of $< 7.5 \times 10^{12}$ G!

In this paper we propose that the spectral bump of the secondary pulse (which corresponds to the polar beam) is caused by cyclotron-resonance reflection of the fan beam by the magnetized photosphere. This leads to a magnetic-field strength of $7 \times 10^{12}(1 + z)$ G, which falls in the range of dipole magnetic fields $(10^{12} - 10^{13}$ G) attributed to AXPs/SGRs in the framework of the fallback-disk scenario.

On the other hand, we stress that the few giant bursts observed from SGRs cannot be explained by any accretion process. The same is true for bursts with large super-Eddington luminosities. They are most likely caused by crustal shifts of plates carrying super-strong magnetic fields $(\gtrsim 10^{15}$ G), as discussed in the classical magnetar literature (e.g. Thomson & Duncan 1995). Our analysis suggests that these events do not take place in the dipole field, but in localized multipole fields. This situation is qualitatively similar to that of the Sun, which shows flare activities in sunspot fields, which are larger than the solar dipole field by at least two orders of magnitude.

In conclusion, our model explains naturally the X-ray spectra and the energy-dependent pulse profiles of 4U 0142+61. Furthermore, it allows this source or any other AXP or SGR to emit big or giant bursts if the neutron star involved sustains multipole fields with strengths in the $10^{14} - 10^{15}$ G range.

References

Alpar, M. A. 2001, ApJ, 554, 1245
Basko, M. M., & Sunyaev, R. A. 1976, MNRAS, 175, 395
Becker, P. A., & Wolff, M. T. 2005, ApJ, 630, 465
Becker, P. A., & Wolff, M. T. 2007, ApJ, 654, 435
Beloborodov, A. M., & Thompson, C. 2007, ApJ, 657, 967
Chatterjee, P., Hernquist, L., & Narayan, R. 2000, ApJ, 534, 373
den Hartog, P. R., Kuiper, L., Hermsen, W., et al. 2008, A&A, 489, 245
Duncan, R. A., & Thompson, C. 1992, ApJ, 392, 9
Ekşi, K. Y., & Alpar, M. A. 2003, ApJ, 599, 450
Enoto, T., Nakazawa, K., Makishima, K. et al. 2010, arXiv:1009.2810
Ertan, Ü., & Alpar, M. A. 2003, ApJ, 593, L93
Ertan, Ü., & Çalışkan, Ş. 2006, ApJ, 649, L87
Ertan, Ü, & Cheng, K. S. 2004, ApJ, 605, 840
Ertan, Ü., Ekşi, K. Y., Erkut, M. H., & Alpar, M. A. 2009, ApJ, 702, 1309
Ertan, Ü., Erkut, M. H., Ekşi, K. Y., & Alpar, M. A. 2007, ApJ, 657, 441
Ertan, Ü., & Erkut, M. H. 2008, ApJ, 673, 1062
Ertan, Ü., Göğüş, E., & Alpar, M.A. 2006, ApJ, 640, 435
Farinelli, R., Titarchuk, L., Paizis, A., & Frontera, F. 2008, ApJ, 680, 602
Fernandez, R., & Thompson, C. 2007, ApJ, 660, 615
Israel, G. L., Angelini, L., Burderi, L., et al. 1999, Nuclear Physics B, 69, 141
Juett, A. M., Marshall, H. L., Chakrabarty, D., & Schulz, N. S. 2002, ApJ, 568, L31
Kaplan, D. L., Chakrabarty, D., Wang, Z., & Wachter, S. 2009, ApJ, 700, 149
Kouveliotou, C., Strohmayer, T., Hurley, K., et al. 1999, ApJ, 510, L115
Kuiper, L., Hermsen, W., den Hartog, R. P. & Collmar, W. 2006, ApJ, 645, 556
Lyutikov, M., & Gavriil, F. P. 2006, MNRAS, 368, 690
Mastichiadis, A., & Kylafis, N. D. 1992, ApJ, 384, 136
Mereghetti, S. 2008, A&Arv, 15, 225
Meszaros, P. 1992, "High-energy Radiation from Magnetized Neutron Stars", The University of Chicago Press
Pavlov, G. G., Shibanov, Y. A., Ventura, J., & Zavlin, V. E. 1994, A&A, 289, 837
Rea, N., Esposito, P., Turolla, R., et al. 2010, arXiv:1010.2781
Thompson, C., & Duncan, R. C. 1995, MNRAS, 275, 255
Thompson, C., Duncan, R. C., Woods, P. M., et al. 2000, ApJ, 543, 340
Trümper, J. E., Zezas, A, Ertan, Ü, & Kylafis, N. D. 2010, A&A, 518, A46
van Paradijs, J., Taam, R. E., & van den Heuvel, E. 1995, A&A, 299, L41
Wang, Z., Chakrabarty, D., & Kaplan, D. L. 2006, Nature, 440, 772
White, N. E., Angelini, L., Ebisawa, K., et al. 1996, ApJ, 463, L83
Wolszczan, A. 1995, Ap&SS, 223, 205
Wolszczan, A. & Frail, D. A. 1992, Nature, 355, 145
Woods, P. M., & Thompson, C. 2006, in "Compact Stellar X-ray Sources", eds. W.H.G. Lewin and M. van der Klis, Cambridge Univ. Press.(astro-ph/0406133)